

Random Inscribed Polytopes Have Similar Radius Functions as Poisson–Delaunay Mosaics*

Herbert Edelsbrunner¹ and Anton Nikitenko¹

¹ IST Austria (Institute of Science and Technology Austria), Am Campus 1, 3400 Klosterneuburg, Austria, edels@ist.ac.at, anton.nikitenko@ist.ac.at

Abstract

Using the geodesic distance on the n -dimensional sphere, we study the expected radius function of the Delaunay mosaic of a random set of points. Specifically, we consider the partition of the mosaic into intervals of the radius function and determine the expected number of intervals whose radii are less than or equal to a given threshold. Assuming the points are not contained in a hemisphere, the Delaunay mosaic is isomorphic to the boundary complex of the convex hull in \mathbb{R}^{n+1} , so we also get the expected number of faces of a random inscribed polytope. We find that the expectations are essentially the same as for the Poisson–Delaunay mosaic in n -dimensional Euclidean space. As proved by Antonelli and collaborators [3], an orthant section of the n -sphere is isometric to the standard n -simplex equipped with the Fisher information metric. It follows that the latter space has similar stochastic properties as the n -dimensional Euclidean space. Our results are therefore relevant in information geometry and in population genetics.

1998 ACM Subject Classification: I.3.5 Computational Geometry and Object Modeling, G.3 Probability and Statistics, G.2 Discrete Mathematics.

2010 AMS Mathematics Subject Classification: 60D05 Geometric probability and stochastic geometry, 68U05 Computer graphics; computational geometry.

Keywords and phrases: Voronoi tessellations, Delaunay mosaics, inscribed polytopes; discrete Morse theory, critical simplices, intervals; stochastic geometry, Poisson point process; Blaschke–Petkantschin formula; Fisher information metric.

1 Introduction

Letting X be a Poisson point process in \mathbb{R}^n , the expected sizes of the Voronoi tessellation and, equivalently, of the dual Delaunay mosaic are reasonably well understood. The starting point for this paper is the question how these expectations change when we pick the points on the n -dimensional sphere, \mathbb{S}^n . Perhaps surprisingly, the difference is very small. Even the partitions of the Delaunay mosaics into the intervals of the respective radius functions are barely distinguishable.

Motivation. Our reason for comparing random sets in the Euclidean space and on the sphere is the Fisher information metric, which measures the dissimilarity between discrete probability distributions. Write $\mathbf{x} = (x_0, x_1, \dots, x_n)$ and $\mathbf{y} = (y_0, y_1, \dots, y_n)$ for two such distributions, with $\sum_{i=0}^n x_i = \sum_{i=0}^n y_i = 1$ and $x_i, y_i \geq 0$ for all i , and note that \mathbf{x} and \mathbf{y} are points of the n -dimensional standard simplex, Δ^n . Letting $\gamma: [0, 1] \rightarrow \Delta^n$ be a smooth curve

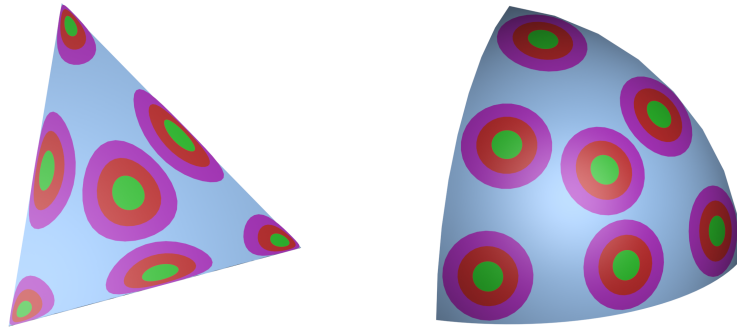
* This work is partially supported by the Austrian Science Fund (FWF), grant no. I02979-N35.

connecting $\mathbf{x} = \gamma(0)$ to $\mathbf{y} = \gamma(1)$, we define its *length* as

$$\text{Length}(\gamma) = \int_{t=0}^1 \sqrt{\frac{1}{2} \sum_{i=0}^n \frac{\dot{\gamma}_i(t)^2}{\gamma_i(t)}} dt, \quad (1)$$

in which $\gamma_i(t)$ and $\dot{\gamma}_i(t)$ are the i -th components of the curve and its velocity vector. The *Fisher information metric* assigns the length of the shortest connecting path to the pair \mathbf{x}, \mathbf{y} ; see [2, Section 2.2] as well as [1, Section I.4], where this metric is referred to as the Shahshahani metric. This way of measuring distance is fundamental in information geometry and in population genetics.

To shed light on the Fisher information metric, we map every point $\mathbf{x} = (x_0, x_1, \dots, x_n)$ of Δ^n to the point $\varphi(\mathbf{x}) = (u_0, u_1, \dots, u_n)$ with $u_i = \sqrt{2x_i}$ for every i . The coordinates of $\varphi(\mathbf{x})$ are all non-negative and satisfy $\sum_{i=0}^n u_i^2 = 2$. In words, $\varphi(\mathbf{x})$ is a point of $\sqrt{2}\mathbb{S}_+^n$, which is our notation for the non-negative orthant of the sphere with radius $\sqrt{2}$ centered at the origin in \mathbb{R}^{n+1} ; see Figure 1 on the right. As noticed already by Antonelli [3], see also Akin [1, page 39], this mapping is an isometry between Δ^n and $\sqrt{2}\mathbb{S}_+^n$. We can therefore understand Δ^n under the Fisher information metric by studying \mathbb{S}_+^n under the geodesic distance. To get a handle on the difference between random sets in \mathbb{R}^n and in Δ^n , we compare point sets selected from Poisson point processes in \mathbb{R}^n and on \mathbb{S}^n , the latter being the topic of this article. Figure 1 illustrates the isometry by showing three level lines each for seven points in the standard triangle on the left and for the seven corresponding points in the positive orthant of the sphere on the right.



■ **Figure 1** *Left*: disk neighborhoods under the Fisher information metric of seven points in the standard triangle. *Right*: the corresponding seven points and cap neighborhoods in the isometric non-negative octant of the 2-sphere. For aesthetic reasons, the octant is scaled to $1/\sqrt{2}$ times its actual size.

Prior work. This article builds on work from three different but related areas: random polytopes, Poisson–Delaunay mosaics, and discrete Morse theory.

Consider the model in which a random polytope is generated by taking the convex hull of randomly chosen points on the unit sphere. The first paper with substantial results on this topic is Miles [17]. The large body of work on the expected number of faces of random polytopes and their volume is summarized and surveyed in [4, 10, 19, 22, 23]. A survey of recent results can be found in [24]. The more general setting in which the points are selected on the boundary of a convex body is addressed in [20], and the linear dependence of the expected number of faces on the number of vertices is proved.

The study of Poisson–Delaunay mosaics in Euclidean space was started by Miles with two seminal papers [16, 17] around 1970. Considering the expected number of k -dimensional simplices in an n -dimensional Poisson–Delaunay mosaic, he settles the question for all values of k in dimensions $n \leq 3$, and for $k = n - 1, n$ in any dimension n . The first substantial extension of these results appeared in [6], settling the question for all values of k in dimension $n = 4$, and determining the density of the radius of a typical simplex. The main new idea in [6] is the classification of the simplices based on the discrete Morse theory of the Delaunay mosaic, and this approach is also central to the work in this paper. Discrete Morse theory was first introduced as an abstract concept in [8], and its generalized version was used in [5] to study the radius function of a Delaunay mosaic.

Concepts and notation. Before stating our results, we introduce some concepts and notation; the detailed description will follow in Section 3. We write \mathbb{R}^n for the n -dimensional Euclidean space, $\mathbb{B}^n \subseteq \mathbb{R}^n$ for the closed unit ball, and $\mathbb{S}^{n-1} = \text{bd } \mathbb{B}^n$ for the unit sphere, the boundary of the unit ball. Following [23], we write ν_n for the n -dimensional volume of \mathbb{B}^n and σ_n for the area (the $(n - 1)$ -dimensional volume) of \mathbb{S}^{n-1} .

To facilitate the comparison between Euclidean and spherical space, we move up by one dimension and consider \mathbb{S}^n , which we equip with the geodesic distance, $d: \mathbb{S}^n \times \mathbb{S}^n \rightarrow \mathbb{R}$, induced by the Euclidean metric in \mathbb{R}^{n+1} ; see Section 3 for more details. The relation between the geodesic distance and the Euclidean distance is $d(x, y) = 2 \arcsin \frac{\|x - y\|}{2}$. Let $\text{Cap}_\eta(x) = \{w \in \mathbb{S}^n \mid d(w, x) \leq \eta\}$ be the spherical cap with center $x \in \mathbb{S}^n$ and geodesic radius $0 \leq \eta \leq \pi$. To measure the area of a cap, we use the Beta function, $B(a, b) = B_1(a, b)$, and its incomplete version, $B_u(a, b) = \int_{t=0}^u t^{a-1} (1-t)^{b-1} dt$, in which $0 \leq u \leq 1$. For $\eta \leq \frac{\pi}{2}$, the fraction of the sphere covered by the cap is $F(\eta) = \frac{1}{2} B_s(\frac{n}{2}, \frac{1}{2}) / B(\frac{n}{2}, \frac{1}{2})$, in which $s = \sin^2 \eta$ is the square of the Euclidean radius measured in \mathbb{R}^{n+1} ; see [14]. The area of the cap is then

$$\text{Area}(\eta) = \begin{cases} F(\eta)\sigma_{n+1} & \text{for } 0 \leq \eta \leq \frac{\pi}{2}, \\ [1 - F(\pi - \eta)]\sigma_{n+1} & \text{for } \frac{\pi}{2} \leq \eta \leq \pi, \end{cases} \quad (2)$$

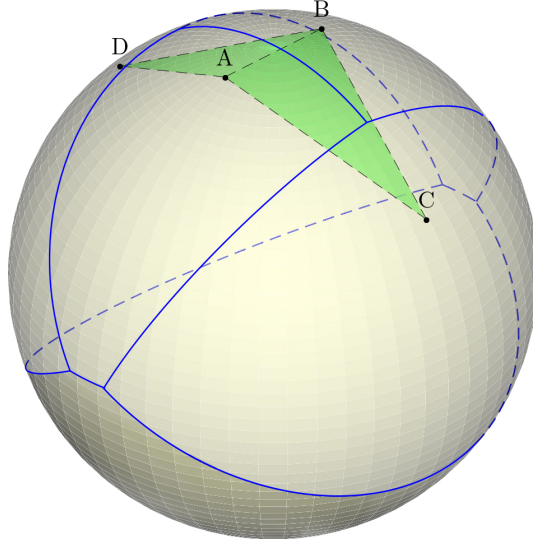
in which $F(\pi - \eta) = F(\eta)$ because $\sin(\pi - \eta) = \sin \eta$. Besides the Beta functions, we will use the Gamma function, $\Gamma(k) = \gamma_\infty(k)$, and its lower incomplete version, $\gamma(k; u) = \int_{t=0}^u t^{k-1} e^{-t} dt$, in which $0 \leq u \leq \infty$. The connection to the Beta functions is $B(a, b) = \Gamma(a)\Gamma(b)/\Gamma(a+b)$. Finally, we write \mathcal{L}_k^n for the Grassmannian, which consists of all k -dimensional planes that pass through the origin in \mathbb{R}^n . This is a manifold of dimension $(n - k) \times k$ and measure $\|\mathcal{L}_k^n\| = \frac{\sigma_n \cdot \sigma_{n-1} \cdots \sigma_{n-k+1}}{\sigma_1 \cdot \sigma_2 \cdots \sigma_k}$; see [23]. This measure appears in the definition of constants that play an important role in the statement of our results:

$$C_{\ell, k}^n = \frac{\sigma_n \cdot \sigma_{n-1} \cdots \sigma_{n-k+1}}{\sigma_1 \cdot \sigma_2 \cdots \sigma_k} \cdot \frac{\Gamma(k)n^{k-1}k!^{n-k}\sigma_k^{k+1}}{(k+1)\sigma_n^k} \cdot E_{\ell, k}^n, \quad (3)$$

$$E_{\ell, k}^n = \mathbb{E}[\text{Vol}(\mathbf{u})^{n-k+1} \mathbf{1}_{k-\ell}(\mathbf{u})], \quad (4)$$

in which $\mathbf{u} = (u_0, u_1, \dots, u_k)$ is a sequence of $k+1$ points chosen independently and uniformly at random on \mathbb{S}^{k-1} , with $\mathbf{1}_{k-\ell}(\mathbf{u}) = 1$, if $k-\ell$ of the $k+1$ facets of the k -simplex span k -planes that separate 0 from \mathbf{u} , and $\mathbf{1}_{k-\ell}(\mathbf{u}) = 0$, otherwise; see [6], where the same constants are studied in more detail.

We follow [21] in defining the Voronoi domain of a point $x \in X$ as the set $\text{Vor}(x)$ of points $w \in \mathbb{S}^n$ that satisfy $d(w, x) \leq d(w, y)$ for all $y \in X$ as well as $d(w, x) < \frac{\pi}{2}$. Note that the Voronoi domains cover \mathbb{S}^n iff there is no closed hemisphere that contains X ; see Figure 2. The Delaunay mosaic is the nerve of the Voronoi domains, which we denote $\text{Del}X$. Assuming general position, $\text{Del}X$ is isomorphic to a subcomplex of the boundary complex of



■ **Figure 2** The Voronoi domains of four points on the 2-dimensional sphere. The darker region in the south does not belong to any of these domains because the four points all belong to the northern hemisphere. The dual Delaunay complex consists of two triangles glued along a shared edge.

$\text{conv } X$ in \mathbb{R}^{n+1} , and it is isomorphic to the entire boundary complex iff X is not contained in any closed hemisphere. Given a geodesic radius $0 \leq \eta \leq \frac{\pi}{2}$, we sometimes restrict the Voronoi domains to $\text{Vor}(x) \cap \text{Cap}_\eta(x)$, for every $x \in X$, and we write $\text{Del}_\eta X$ for the nerve of the thus restricted Voronoi domains. The (*geodesic*) *radius function*, $\mathcal{R}: \text{Del}X \rightarrow \mathbb{R}$, maps every Delaunay simplex to the radius of its *smallest empty circumscribed cap*; see details in Section 3. By assumption, this radius is always less than $\frac{\pi}{2}$, and we observe that $\mathcal{R}^{-1}[0, \eta] = \text{Del}_\eta X$ for all $\eta \geq 0$. For points in general position, \mathcal{R} is a generalized discrete Morse function, as defined in [5, 8], which implies a partition of $\text{Del}X$ into maximal *intervals* $[L, U] = \{Q \mid L \subseteq Q \subseteq U\}$ consisting of simplices with equal function value, as discussed in Section 3. The *type* of the interval $[L, U]$ is (ℓ, k) , in which $\ell = \dim L$ and $k = \dim U$. If $L = U$, then the interval contains a single simplex, which we call a *critical simplex* of \mathcal{R} .

We need one more concept to express the asymptotic behavior of the expected numbers, when their density goes to infinity. Assuming a Poisson point process with density $\rho > 0$ on \mathbb{S}^n , for a cap with geodesic radius η , we call $\bar{\eta} = \eta\rho^{1/n}$ the *normalized radius* of the cap. It is the geodesic radius of the cap after scaling the unit sphere to the sphere with area $\rho\sigma_n$.

Results. Our main result concerns the radius function on the Delaunay mosaic. For each type, we express the expected number of intervals of that type with normalized radius smaller than a threshold in terms of an integral, which we evaluate asymptotically, when the density of the Poisson point process goes to infinity.

► **Theorem 1 (Main Result).** *Let X be a Poisson point process with density $\rho > 0$ on \mathbb{S}^n . For any integers $1 \leq \ell \leq k \leq n$ and any real number $0 < \eta_0 < \frac{\pi}{2}$, the expected number of intervals of type (ℓ, k) and geodesic radius at most η_0 is*

$$\mathbb{E}[c_{\ell,k}^n, \eta_0] = \rho\sigma_{n+1} \cdot \frac{\sigma_n^k}{2\Gamma(k)n^{k-1}} \cdot C_{\ell,k}^n \int_{t=0}^s \rho^k t^{\frac{kn-2}{2}} (1-t)^{\frac{n-k-1}{2}} \mathbb{P}_0(\sqrt{t}) dt, \quad (5)$$

in which $s = \sin^2 \eta_0$ is the square of the maximum Euclidean radius, and $\mathbb{P}_\emptyset(r)$ is the probability that a spherical cap with geodesic radius $\eta = \arcsin r$ contains no points of X , namely $\mathbb{P}_\emptyset(r) = e^{-\rho \text{Area}(\eta)}$. Let now $\rho \rightarrow \infty$. For any $\bar{\eta}_0 \in [0, +\infty]$, the expected number of intervals of type (ℓ, k) and normalized radius at most $\bar{\eta}_0$ is

$$\mathbb{E}[c_{\ell,k}^n, \bar{\eta}_0] = \rho \sigma_{n+1} \cdot \frac{\gamma(k;v)}{\Gamma(k)} \cdot C_{\ell,k}^n + o(\rho), \quad (6)$$

in which $v = \bar{\eta}_0^n \nu_n$ is the volume of the n -ball with radius $\bar{\eta}_0$.

REMARKS. (1A) Theorem 1 does not cover the case $\ell = 0$, i.e., intervals containing vertices, but here the results are straightforward. Specifically, the expected number of critical vertices is $\mathbb{E}[c_{0,0}^n, \eta_0] = \rho \sigma_{n+1}$, for every $\eta_0 \geq 0$, and $c_{0,k}^n = 0$ for every $k \geq 1$.

(1B) We will prove that for constant s , the integral in (5) is bounded away from both 0 and ∞ . This implies that the expected number of intervals in (5) is of order $\Theta(\rho)$; compare with [20].

(1C) We will also prove that setting $\bar{\eta}_0 = \infty$ in (6) gives the total number of intervals of type (ℓ, k) as $\mathbb{E}[c_{\ell,k}^n] = \rho \sigma_{n+1} \cdot C_{\ell,k}^n + o(\rho)$. On the other hand, letting $\bar{\eta}_0 \rightarrow \infty$, we get the total number of intervals of geodesic radius $\Theta(\rho^{-1/n})$. This implies that the number of intervals with radius $\omega(\rho^{-1/n})$ is $o(\rho)$. Note that also the number of intervals with radius $o(\rho^{-1/n})$ is $o(\rho)$.

The total number of simplices of dimension j in the Delaunay mosaic is easy to deduce from the number of intervals: $d_j^n = \sum_{k=j}^n \sum_{\ell=0}^j \binom{k-\ell}{k-j} c_{\ell,k}^n$. Accordingly, we define the constant $D_j^n = \sum_{k=j}^n \sum_{\ell=0}^j \binom{k-\ell}{k-j} C_{\ell,k}^n$. We generalize this relation so it depends on a normalized radius threshold:

► **Corollary 2** (Delaunay Simplices). *Let X be a Poisson point process with density $\rho > 0$ on \mathbb{S}^n . For any integer $j \geq 1$ and any non-negative real number $\bar{\eta}_0$, the expected number of j -simplices of $\text{Del}X$ with normalized radius at most $\bar{\eta}_0$ is*

$$\mathbb{E}[d_j^n, \bar{\eta}_0] = \rho \sigma_{n+1} \cdot \sum_{k=j}^n \frac{\gamma(k;v)}{\Gamma(k)} \sum_{\ell=0}^j \binom{k-\ell}{k-j} C_{\ell,k}^n + o(\rho), \quad (7)$$

in which $v = \bar{\eta}_0^n \nu_n$. Setting

$$G_j^n(\bar{\eta}_0) = \sum_{k=j}^n \frac{\gamma(k;v)}{\Gamma(k)} \sum_{\ell=0}^j \binom{k-\ell}{k-j} \frac{C_{\ell,k}^n}{D_j^n}, \quad (8)$$

we thus get the distribution of the normalized radius of the typical j -simplex in the limit when $\rho \rightarrow \infty$.

REMARKS. (2A) Observe that $\rho \sigma_{n+1}$ is the expected number of points in X . Comparing with [6], we thus notice that (6), (7), and (8) are essentially the same expressions as for the Poisson point process in \mathbb{R}^n . This justifies the title of this article.

(2B) While we state our results for Poisson point processes, very similar results can be obtained for the uniform distribution; see Appendix A.

Outline. Section 2 introduces the main technical tool used to prove our results. Section 3 gives the background, including discrete Morse theory. Section 4 proves the integral equation and the asymptotic result both stated in Theorem 1. Section 5 concludes the paper.

2 Blaschke–Petkantschin Formula for the Sphere

This section introduces a formula of Blaschke–Petkantschin type used in the proof of Theorem 1. Since it is a stand-alone result, not specific to the problem addressed in this article, we present it before discussing the background related to the subject in this paper. In its basic form, the *Blaschke–Petkantschin formula* writes an integral over \mathbb{R}^{n+1} as an integral over the Grassmannian, \mathcal{L}_k^{n+1} . We adapt the original such formula to the n -sphere. Formulas of this type were studied in [26]. To express the result, we write P^\perp for the $(n - k + 1)$ -plane orthogonal to the k -plane P , both passing through the origin in \mathbb{R}^{n+1} , and we write S_P for the unit $(k - 1)$ -sphere in P . As usual, we use boldface to denote sequences of points: $\mathbf{x} = (x_0, x_1, \dots, x_k)$, etc. A shortcut $p + r\mathbf{u}$ is used for $(p + ru_0, p + ru_1, \dots, p + ru_k)$. The integrations are with respect to the standard measure on the Grassmanian and the Lebesgue measures in the plane and on the sphere.

► **Theorem 3** (Blaschke–Petkantschin for the Sphere). *Let n be a positive integer, $1 \leq k \leq n$, and $f: (\mathbb{S}^n)^{k+1} \rightarrow \mathbb{R}$ a non-negative measurable function. Then*

$$\int_{\mathbf{x} \in (\mathbb{S}^n)^{k+1}} f(\mathbf{x}) \, d\mathbf{x} = \int_{P \in \mathcal{L}_k^{n+1}} \int_{p \in P^\perp} r^{kn-2} \int_{\mathbf{u} \in (S_P)^{k+1}} f(p + r\mathbf{u}) [k! \text{Vol}(\mathbf{u})]^{n-k+1} \, d\mathbf{u} \, dp \, dP, \quad (9)$$

in which $r^2 = 1 - \|p\|^2$, implicitly assuming $\|p\| \leq 1$, and $\text{Vol}(\mathbf{u})$ is the k -dimensional volume of the convex hull of the points in \mathbf{u} , which is a k -simplex. If f is rotationally symmetric, we define $f_r(\mathbf{u}) = f(p + r\mathbf{u})$, in which \mathbf{u} is a k -simplex on $\mathbb{S}^{k-1} \subseteq \mathbb{R}^k$, and p is any point with $\|p\|^2 = 1 - r^2 \leq 1$ in the $(n - k + 1)$ -plane orthogonal to $\mathbb{R}^k \subseteq \mathbb{R}^{n+1}$. With this notation, we have

$$\int_{\mathbf{x} \in (\mathbb{S}^n)^{k+1}} f(\mathbf{x}) \, d\mathbf{x} = \frac{\sigma_{n+1}}{2} \|\mathcal{L}_k^n\| \int_{t=0}^1 t^{\frac{kn-2}{2}} (1-t)^{\frac{n-k-1}{2}} \int_{\mathbf{u} \in (\mathbb{S}^{k-1})^{k+1}} f_{\sqrt{t}}(\mathbf{u}) [k! \text{Vol}(\mathbf{u})]^{n-k+1} \, d\mathbf{u} \, dt. \quad (10)$$

Proof. We first argue that f may be assumed to be continuous. Consider the subset M of $\mathcal{L}_k^{n+1} \times \mathbb{R}^{n+1} \times (\mathbb{R}^{n+1})^{k+1}$ consisting of all triplets (P, p, \mathbf{u}) such that $p \in P^\perp$, $\|p\| < 1$, and $\mathbf{u} \in (S_P)^{k+1}$. Clearly, M is a submanifold of the product space with a natural measure. Recall that $r^2 = 1 - \|p\|^2$ and consider the mapping $T: M \rightarrow (\mathbb{S}^n)^{k+1}$ defined by $T(P, p, \mathbf{u}) = p + r\mathbf{u}$. It is a bijection up to a set of measure 0. By Theorem 20.3 in [9], there exists a corresponding Jacobian $J: M \rightarrow \mathbb{R}$, meaning that every integrable function f satisfies $\int_{\mathbf{x} \in (\mathbb{S}^n)^{k+1}} f(\mathbf{x}) \, d\mathbf{x} = \int_{y \in M} f(T(y)) J(y) \, dy$. For non-negative f , the right-hand side integral can be split using Fubini's theorem. The existence of the Jacobian is thus settled, and to find its values, we may assume that f be continuous.

The main idea in the rest of the proof is to thicken \mathbb{S}^n to an $(n + 1)$ -dimensional annulus, to apply the original Blaschke–Petkantschin formula to this annulus, and to take the limit when we shrink the annulus back to \mathbb{S}^n . We write $\mathbb{A}_{1+\varepsilon}^{n+1} = (1 + \varepsilon)\mathbb{B}^{n+1} \setminus \text{int } \mathbb{B}^{n+1}$ for the $(n + 1)$ -dimensional annulus with inner radius 1 and outer radius $1 + \varepsilon$. We begin by extending f from the sphere to the annulus. Specifically, for points $y_i \in \mathbb{A}_{1+\varepsilon}^{n+1}$, we set

$$F(y_0, y_1, \dots, y_k) = f(y_0/\|y_0\|, y_1/\|y_1\|, \dots, y_k/\|y_k\|). \quad (11)$$

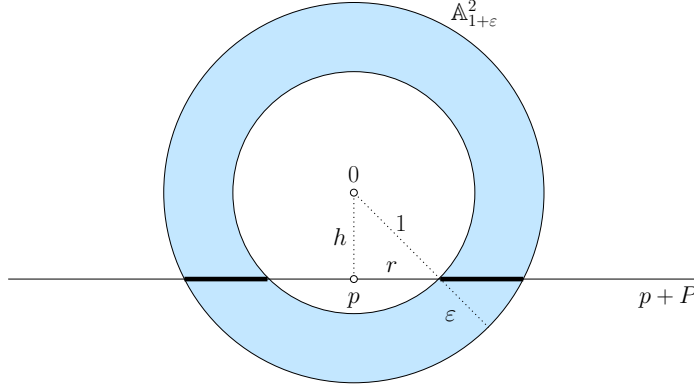
Since f is continuous on the $(k + 1)$ -fold product of spheres, by assumption, F is continuous on the $(k + 1)$ -fold product of annuli. Because F is continuous on a compact set and therefore

bounded and uniformly continuous, we have

$$\int_{\mathbf{x} \in (\mathbb{S}^n)^{k+1}} f(\mathbf{x}) \, d\mathbf{x} = \lim_{\varepsilon \rightarrow 0} \frac{1}{\varepsilon^{k+1}} \int_{\mathbf{y} \in (\mathbb{A}_{1+\varepsilon}^{n+1})^{k+1}} F(\mathbf{y}) \, d\mathbf{y} \quad (12)$$

$$= \lim_{\varepsilon \rightarrow 0} \frac{1}{\varepsilon^{k+1}} \int_{P \in \mathcal{L}_k^{n+1}} \int_{p \in P^\perp} \int_{\mathbf{u} \in A^{k+1}} F(\mathbf{u}) [k! \text{Vol}(\mathbf{u})]^{n-k+1} \, d\mathbf{u} \, dp \, dP, \quad (13)$$

in which $A = \mathbb{A}_{1+\varepsilon}^{n+1} \cap [p+P]$ is the k -dimensional slice of the $(n+1)$ -dimensional annulus defined by P and p . We obtain (13) from (12) by applying the standard Blaschke–Petkantschin formula in \mathbb{R}^{n+1} to the function $F(\mathbf{y})$ times the indicator function of the $(k+1)$ -fold product of annuli, and then absorb the indicator into the integration domain. To continue, we investigate the slice of the annulus whose $(k+1)$ -fold product is the innermost integration domain; see Figure 3. Write $h = \|p\|$ for the height of the slice, which is non-empty for $0 \leq h \leq 1 + \varepsilon$. A is a (possibly degenerate) k -dimensional annulus, with squared inner radius $r^2 = \max\{0, 1 - h^2\}$ and squared outer radius $r_\varepsilon^2 = (1 + \varepsilon)^2 - h^2$. We split the integration domain into three regions: $h \leq 1 - \varepsilon^{0.2}$, $1 - \varepsilon^{0.2} < h \leq 1$, and $1 < h \leq 1 + \varepsilon$.



■ **Figure 3** For $h = \|p\| < 1$, the slice of the $(n+1)$ -dimensional annulus is a k -dimensional annulus. In this picture, $n+1 = 2$ and $k = 1$.

We first show that the contribution of the region $1 - \varepsilon^{0.2} < h \leq 1$ is small. To get started, note that $r_\varepsilon - r = (r_\varepsilon^2 - r^2)/(r_\varepsilon + r) = (2\varepsilon + \varepsilon^2)/(r_\varepsilon + r)$. For small ε , this implies $r_\varepsilon - r \leq \text{const} \cdot \varepsilon/r_\varepsilon$, in which we deliberately avoid the computation of the constant. With this, we can bound the k -dimensional volume of A . Assuming $k \geq 2$, we get $\text{Vol}(A) = \nu_k(r_\varepsilon^k - r^k) = \nu_k(r_\varepsilon - r)(r_\varepsilon^{k-1} + r_\varepsilon^{k-2}r + \dots + r^{k-1}) \leq \text{const} \cdot \varepsilon r_\varepsilon^{k-2}$, in which the constant depends only on k and n . As noted before, the inequality also holds for $k = 1$. Since $h > 1 - \varepsilon^{0.2}$, we also get $r_\varepsilon^2 < (1 + \varepsilon)^2 - (1 - \varepsilon^{0.2})^2 \leq \varepsilon^2 + 2\varepsilon + 2\varepsilon^{0.2} - \varepsilon^{0.4}$ for small ε , which implies $r_\varepsilon < \text{const} \cdot \varepsilon^{0.1}$. Clearly, the k -dimensional volume of any k -simplex with vertices inside A can not exceed a constant times the k -th power of the diameter of A , which is $2r_\varepsilon$, implying $\text{Vol}(\mathbf{u}) \leq \text{const} \cdot r_\varepsilon^k$. Recalling that F is bounded, we thus get

$$\left| \int_{P \in \mathcal{L}_k^{n+1}} \int_{\substack{p \in P^\perp \\ \|p\| < 1 - \varepsilon^{0.2}}} \frac{1}{\varepsilon^{k+1}} \int_{\mathbf{u} \in A^{k+1}} F(\mathbf{u}) [k! \text{Vol}(\mathbf{u})]^{n-k+1} \, d\mathbf{u} \, dp \, dP \right| \quad (14)$$

$$\leq \text{const} \int_{h=1-\varepsilon^{0.2}}^1 \frac{1}{\varepsilon^{k+1}} \text{Vol}(A)^{k+1} \text{Vol}(\mathbf{u})^{n-k+1} dh \quad (15)$$

$$\leq \text{const} \int_{h=1-\varepsilon^{0.2}}^1 \frac{1}{\varepsilon^{k+1}} (\varepsilon r_\varepsilon^{k-2})^{k+1} r_\varepsilon^{k(n-k+1)} dh \quad (16)$$

$$\leq \text{const} \int_{h=1-\varepsilon^{0.2}}^1 r_\varepsilon^{kn-2} dh \leq \text{const} \cdot \varepsilon^{0.2} \cdot \varepsilon^{0.1(kn-2)} \rightarrow 0. \quad (17)$$

Here we use the bound on r_ε for the last inequality, and $kn \geq 1$ to see that the expression tends to zero. Next consider the region $1 < h \leq 1 + \varepsilon$, in which A is a ball of radius r_ε , so $\text{Vol}(A) = \nu_k r_\varepsilon^k$. We have $\text{Vol}(\mathbf{u}) \leq \nu_k r_\varepsilon^k$, as before, and $r_\varepsilon^2 \leq (1 + \varepsilon)^2 - 1$, which implies $r_\varepsilon \leq \text{const} \cdot \sqrt{\varepsilon}$. With this, we can again establish the vanishing of the integral as $\varepsilon \rightarrow 0$:

$$\left| \int_{P \in \mathcal{L}_k^{n+1}} \int_{\substack{p \in P^\perp \\ 1 \leq \|p\| \leq 1+\varepsilon}} \int_{u \in A^{k+1}} \frac{1}{\varepsilon^{k+1}} F(\mathbf{u}) [k! \text{Vol}(\mathbf{u})]^{n-k+1} d\mathbf{u} dp dP \right| \quad (18)$$

$$\leq \text{const} \int_{h=1}^{1+\varepsilon} \frac{1}{\varepsilon^{k+1}} \text{Vol}(A)^{k+1} \text{Vol}(\mathbf{u})^{n-k+1} dh \quad (19)$$

$$\leq \text{const} \int_{h=1}^{1+\varepsilon} \frac{1}{\varepsilon^{k+1}} r_\varepsilon^{k(n+2)} dh \leq \text{const} \cdot \varepsilon \cdot \varepsilon^{(kn-2)/2} \rightarrow 0. \quad (20)$$

We have thus established that the relevant region is $0 \leq h \leq 1 - \varepsilon^{0.2}$, and we are ready to investigate its contribution. First, we claim that the width of the annulus A is

$$r_\varepsilon - r = r \sqrt{1 + \frac{2\varepsilon + \varepsilon^2}{r^2}} - r = \frac{\varepsilon}{r} + o(\varepsilon). \quad (21)$$

To get the right-hand side of (21), we use the Taylor expansion of $g(x) = (1+x)^{1/2} = 1 + \frac{1}{2}x - \frac{1}{8}x^2 + \dots$, and $r > \varepsilon^{0.1}$ as well as $x = (2\varepsilon + \varepsilon^2)/r^2 < 3\varepsilon^{0.8}$, which we get from the assumed $h \leq 1 - \varepsilon^{0.2}$. Observing that $\varepsilon^2/(2r^2) = O(\varepsilon^{1.8})$, we get $rg(x) - r = \frac{\varepsilon}{r} + O(r\varepsilon^{1.8}) + O(r\varepsilon^{1.6})$ and therefore (21). Using the fact that $F(\mathbf{u})$ is equal to $f(\mathbf{u})$ when all points lie on the inner sphere and the uniform continuity of F and writing S_r for the $(k-1)$ -sphere with center p and radius r in $P \in \mathcal{L}_k^{n+1}$, we get

$$\int_{\mathbf{u} \in A^{k+1}} \frac{1}{\varepsilon^{k+1}} F(\mathbf{u}) [k! \text{Vol}(\mathbf{u})]^{n-k+1} d\mathbf{u} = \left(\frac{1}{r}\right)^{k+1} \int_{\mathbf{u} \in (S_r)^{k+1}} f(\mathbf{u}) [k! \text{Vol}(\mathbf{u})]^{n-k+1} d\mathbf{u} + o(1), \quad (22)$$

in which the integration domain on the right is the k -fold product of the $(k-1)$ -sphere with center p and radius r in P , and $o(1)$ is uniform over p and P . Substituting (17), (20), and

(22) into (13), we finally get

$$\int_{\mathbf{x} \in (\mathbb{S}^n)^{k+1}} f(\mathbf{x}) \, d\mathbf{x} \quad (23)$$

$$= \lim_{\varepsilon \rightarrow 0} \int_{P \in \mathcal{L}_k^{n+1}} \int_{\substack{p \in P^\perp \\ \|p\| \leq 1 - \varepsilon^{0.2}}} \left[\frac{1}{r^{k+1}} \int_{\mathbf{u} \in (S_r)^{k+1}} f(\mathbf{u}) [k! \text{Vol}(\mathbf{u})]^{n-k+1} \, d\mathbf{u} + o(1) \right] dp \, dP + o(1) \quad (24)$$

$$= \int_{P \in \mathcal{L}_k^{n+1}} \int_{p \in P^\perp} \left(\frac{1}{r}\right)^{k+1} \int_{\mathbf{u} \in (S_r)^{k+1}} f(\mathbf{u}) [k! \text{Vol}(\mathbf{u})]^{n-k+1} \, d\mathbf{u} \, dp \, dP \quad (25)$$

$$= \int_{P \in \mathcal{L}_k^{n+1}} \int_{p \in P^\perp} r^{kn-2} \int_{\mathbf{u} \in (S_P)^{k+1}} f(p + r\mathbf{u}) [k! \text{Vol}(\mathbf{u})]^{n-k+1} \, d\mathbf{u} \, dp \, dP, \quad (26)$$

in which we drop the $\|p\| \leq 1 - \varepsilon^{0.2}$ condition in (24) for the implicitly assumed $\|p\| \leq 1$ when passing to (25), which we can do because the difference vanishes in the limit and (26) is obtained by rescaling and translating the sphere in (25). Indeed, the power of r is a consequence of scaling the volume of the k -simplex, adjusting the volume of the integration domain, and subtracting the power we have already in (25): $k(n - k + 1) + (k - 1)(k + 1) - (k + 1) = kn - 2$. This proves the first relation claimed in Theorem 3.

To get the second relation, we simplify the first by exploiting the rotational symmetry of f . Recalling that $r^2 = 1 - \|p\|^2$, it makes sense to define $f_r(\mathbf{u}) = f(p + r\mathbf{u})$ on the $(k + 1)$ -fold product of $S_P \subseteq \mathbb{S}^n$ because the direction of p does not matter for a fixed height. Neither does P influence the function for a fixed height, so we can define f_r on $(\mathbb{S}^{k-1})^{k+1}$. Thus

$$\int_{\mathbf{x} \in (\mathbb{S}^n)^{k+1}} f(\mathbf{x}) \, d\mathbf{x} = \|\mathcal{L}_k^{n+1}\| \int_{p \in \mathbb{B}^{n-k+1}} r^{kn-2} \int_{\mathbf{u} \in (\mathbb{S}^{k-1})^{k+1}} f_r(\mathbf{u}) [k! \text{Vol}(\mathbf{u})]^{n-k+1} \, d\mathbf{u} \, dp \quad (27)$$

$$= \|\mathcal{L}_k^{n+1}\| \sigma_{n-k+1} \int_{h=0}^1 h^{n-k} r^{kn-2} \int_{\mathbf{u} \in (\mathbb{S}^{k-1})^{k+1}} f_r(\mathbf{u}) [k! \text{Vol}(\mathbf{u})]^{n-k+1} \, d\mathbf{u} \, dh \quad (28)$$

$$= \frac{\sigma_{n+1}}{2} \|\mathcal{L}_k^n\| \int_{t=0}^1 t^{\frac{kn-2}{2}} (1-t)^{\frac{n-k-1}{2}} \int_{\mathbf{u} \in (\mathbb{S}^{k-1})^{k+1}} f_r(\mathbf{u}) [k! \text{Vol}(\mathbf{u})]^{n-k+1} \, d\mathbf{u} \, dt, \quad (29)$$

in which $t = r^2 = 1 - h^2$. We get (27) from (26) because every $P \in \mathcal{L}_k^{n+1}$ contributes the same to the integral. Similarly, we get (28) from (27) by integrating over the range of heights and compensating for the different sizes of the corresponding spheres, aka expressing the integral in polar coordinates. Finally, we get (29) from (28) by substituting t for r^2 , $1 - t$ for h^2 , and dt for $-2h \, dh$, noting that the minus sign is absorbed by reversing the limits of integration. This proves the second relation in Theorem 3. ◀

3 Background

This section introduces the geometric background needed to appreciate the results in this paper. After presenting the diagrams under study, we explain the connection to discrete Morse theory, and finally describe how we generate random diagrams.

Voronoi tessellations and Delaunay mosaics. We recall that the object under consideration is $\mathbb{S}^n \subseteq \mathbb{R}^{n+1}$ with the *geodesic distance*, $d: \mathbb{S}^n \times \mathbb{S}^n \rightarrow \mathbb{R}$, the metric inherited from the Euclidean metric on \mathbb{R}^{n+1} . The distance between any pair of points is defined to be the length of the shortest connecting path: $d(x, y) = 2 \arcsin \frac{\|x-y\|}{2}$. This shortest path is unique, unless $y = -x$, in which case there are infinitely many shortest paths of length π . Letting X be a finite set of points on \mathbb{S}^n , we define the *Voronoi domain* of $x \in X$ as the points for which x minimizes the geodesic distance, further constraining it to within the open hemisphere centered at x :

$$\text{Vor}(x) = \{w \in \mathbb{S}^n \mid d(w, x) \leq d(w, y) \text{ for all } y \in X \text{ and } d(w, x) < \frac{\pi}{2}\}. \quad (30)$$

Note that $d(w, x) \leq d(w, y)$ defines a closed hemisphere, namely all points $w \in \mathbb{S}^n$ that satisfy $\|w - x\| \leq \|w - y\|$ in \mathbb{R}^{n+1} . It follows that $\text{Vor}(x)$ is the intersection of a finite collection of hemispheres — a set we refer to as a (*convex*) *spherical polytope*. Any two of these spherical polytopes have disjoint interiors. The *Voronoi tessellation* of X is the collection of Voronoi domains, one for each point in X . It covers the entire n -sphere, except if X is contained in a closed hemisphere, in which case it covers \mathbb{S}^n minus a possibly degenerate but non-empty spherical polytope; see Figure 2. Generically, the common intersection of $1 \leq k \leq n + 1$ Voronoi domains is either empty or a shared face of dimension $n - k + 1$, and the common intersection of $n + 2$ or more Voronoi domains is empty. The *Delaunay mosaic* of X is isomorphic to the nerve of the Voronoi tessellation:

$$\text{Del}X = \{Q \subseteq X \mid \bigcap_{x \in Q} \text{Vor}(x) \neq \emptyset\}. \quad (31)$$

The Nerve Theorem [13] implies that the Delaunay mosaic has the same homotopy type as the union of Voronoi domains. Assuming there is no closed hemisphere that contains all points, this is the homotopy type of \mathbb{S}^n .

Delaunay mosaics and inscribed polytopes. The Delaunay mosaic is an (abstract) simplicial complex. In the generic case, $\text{Del}X$ can be geometrically realized in \mathbb{R}^{n+1} , namely by mapping every abstract simplex, Q , to the convex hull of its points. To make this precise, we compare $\text{Del}X$ with the boundary complex of $\text{conv} X$, which is a convex polytope inscribed in the n -sphere. Each $(n - 1)$ -sphere $S \subseteq \mathbb{S}^n$ defines two (closed) caps. If S is a great-sphere, these caps are hemispheres, else they have different volume and we call one the *small cap* and the other the *big cap*. Every facet of $\text{conv} X$ defines such a pair of caps, namely the portions of \mathbb{S}^n on the two sides of the n -plane spanned by the facet. One of these caps is *empty*, by which we mean that no point of X lies in its interior. If 0 is in the interior of $\text{conv} X$, then all empty caps are small, but if $0 \notin \text{conv} X$, then there is at least one empty big cap. For non-generic sets, 0 may lie on the boundary of $\text{conv} X$, in which case there is at least one empty hemisphere cap. Parsing the definitions in (30) and (31), we observe that a simplex $Q \subseteq X$ belongs to the Delaunay mosaic iff there is an $(n - 1)$ -sphere, S , that contains Q , is not a great-sphere, and whose empty cap is small. In the generic case, these simplices Q are exactly the faces of the facets of $\text{conv} X$ whose small caps are empty. In particular, it shows that if points are not contained in any hemisphere, then $\text{Del}X$ is isomorphic to $\text{conv} X$, a random inscribed polytope.

Radius function. Consider growing a spherical cap from each point in X . To formalize this process, we recall that $\text{Cap}_\eta(x) = \{w \in \mathbb{S}^n \mid d(w, x) \leq \eta\}$ is the cap with center $x \in X$ and geodesic radius η . Clipping the Voronoi domain to within the cap, for each point $x \in X$,

we get a subcomplex of the Delaunay mosaic when we take the nerve:

$$\text{Del}_\eta X = \{Q \subseteq X \mid \bigcap_{x \in Q} [\text{Vor}(x) \cap \text{Cap}_\eta(x)] \neq \emptyset\}. \quad (32)$$

By construction, $\text{Del}_\eta X$ is a simplicial complex, which we call the *Delaunay complex*, and $\text{Del}_\eta X \subseteq \text{Del}_\zeta X$ whenever $\eta \leq \zeta$. For $\eta = \frac{\pi}{2}$, each restricting cap is a hemisphere and thus contains its corresponding Voronoi domain, which implies $\text{Del}_{\pi/2} X = \text{Del} X$. We are now ready to introduce the *radius function*, $\mathcal{R}: \text{Del} X \rightarrow \mathbb{R}$, which maps every simplex to the smallest geodesic radius for which the simplex belongs to the subcomplex of the Delaunay mosaic:

$$\mathcal{R}(Q) = \min\{\eta \mid Q \in \text{Del}_\eta X\}. \quad (33)$$

In other words, $\mathcal{R}^{-1}[0, \eta] = \text{Del}_\eta X$. This definition is different from but equivalent to the one we gave in the introduction. We will prove shortly that for generic X , the radius function on the Delaunay mosaic is a generalized discrete Morse function; see [5, 8]. To explain what this means, we let $L \subseteq U$ be two simplices in $\text{Del} X$, and we call $[L, U] = \{Q \mid L \subseteq Q \subseteq U\}$ an *interval* and (ℓ, k) with $\ell = \dim L$ and $k = \dim U$ its *type*. For simple combinatorial reasons, the number of simplices in $[L, U]$ is $2^{k-\ell}$. A function $g: \text{Del} X \rightarrow \mathbb{R}$ is a *generalized discrete Morse function* if there exists a partition of $\text{Del} X$ into intervals such that $g(P) \leq g(Q)$ whenever $P \subseteq Q$, with equality in this case iff P and Q belong to the same interval. We can prove that the radius function for a generic set X satisfies this condition. Formally, we say a finite set $X \subseteq \mathbb{S}^n$ is in *general position* if $|X| > n + 1$ and for every $0 \leq k < n$

1. no $k + 3$ points of X belong to a common k -sphere on \mathbb{S}^n ,
2. considering the unique $(k + 1)$ -sphere that passes through $k + 3$ points of X , no $k + 2$ of these points belong to a common k -sphere that shares its center with the $(k + 1)$ -sphere.

Condition 2 implies that no $n + 1$ points of X lie on a great-sphere of \mathbb{S}^n . We need a few additional concepts. Assume X is in general position and $Q \subseteq X$ is a k -simplex with $0 \leq k \leq n$. A cap *circumscribes* Q if the bounding $(n - 1)$ -sphere passes through all points of Q . Since X is generic, Q has a unique *smallest circumscribed cap*, which we denote $\text{cap}(Q)$. If $Q \in \text{Del} X$, Q also has a unique *smallest empty circumscribed cap*, which may or may not be the smallest circumscribed cap. We call it the *circumcap* of Q and denote it as $\text{cap}_\emptyset(Q)$. The *Euclidean center* of a cap is the center of the bounding $(n - 1)$ sphere, which is a point in \mathbb{R}^{n+1} but not on \mathbb{S}^n . Using this center, we introduce a notion of visibility within the affine hull of Q , which is a k -dimensional plane in \mathbb{R}^{n+1} . Recalling that a facet of k -simplex is a $(k - 1)$ -dimensional face, we say a facet of Q is *visible* from this center if the $(k - 1)$ -plane spanned by the facet separates the center from Q or, equivalently, if the center lies in one closed k -dimensional halfspace bounded by the $(k - 1)$ -plane and Q is contained in the other such halfspace.

► **Lemma 4 (Radius Function).** *Let $X \subseteq \mathbb{S}^n$ be finite and in general position. Then $\mathcal{R}: \text{Del} X \rightarrow \mathbb{R}$ is a generalized discrete Morse function, and $[L, U]$ is an interval of \mathcal{R} iff $\text{cap}(U)$ is empty and L is the maximal common face of all facets of U that are visible from the Euclidean center of $\text{cap}(U)$. Furthermore, for every $Q \in [L, U]$, we have $\text{cap}_\emptyset(Q) = \text{cap}(U)$.*

Proof. We prove that for each $Q \in \text{Del} X$ there are unique Delaunay simplices $L \subseteq Q \subseteq U$ such that $\text{cap}(U) = \text{cap}_\emptyset(U)$, L is the intersection of all visible facets of U , and all simplices in $[L, U]$ share the circumcap. Note that $\mathcal{R}(Q)$ is the geodesic radius of the circumcap of Q . Letting $U \subseteq X$ be the set of all points on the $(n - 1)$ -sphere that bounds this circumcap,

we have $\text{cap}_\emptyset(U) = \text{cap}(U)$ for else we could find a smaller empty circumscribed cap. Let z be the center and η the geodesic radius of $\text{cap}(U)$. By assumption of general position, $|U| \leq n + 1$, so U is a Delaunay simplex. For every facet F of U , let z_F be the center and η_F the geodesic radius of $\text{cap}(F)$, and let u_F be the unique vertex in $U \setminus F$. We move the center of this cap along the shortest path from z_F to z while adjusting the radius so that all points of F remain on the boundary of the cap. During this motion, the radius increases continuously, and when it reaches η , the boundary of the cap passes through u_F . If F is visible from z , then u_F is inside the cap at the beginning and on the boundary of the cap at the end of the motion. If F is not visible from the Euclidean center, then u_F changes from outside at the beginning to on the boundary of the cap at the end of the motion. In other words, $\text{cap}(U)$ is the circumcap of every visible facet of U , but every invisible facet has a smaller empty circumscribed cap. Since the intersection of two simplices with common circumcap has the same circumcap [5, Lemma 3.4], we can take L as the intersection of all visible facets of U and get $\text{cap}_\emptyset(L) = \text{cap}(U)$. On the other hand, any face of U that does not contain L is also a face of an invisible facet and therefore has a smaller empty circumscribed cap. This implies $L \subseteq Q$.

We note that the construction gives a partition of $\text{Del}X$ into intervals. Indeed, any two Delaunay simplices sharing the circumcap give rise to the same simplex U and therefore to the same interval $[L, U]$. This concludes the proof. \blacktriangleleft

REMARK. (4A) While the proof follows almost verbatim the proof in the Euclidean case [5], and actually the Euclidean Delaunay mosaic of the spherical point set is almost identical to the one we are talking about, there is a subtlety hidden in its definition. Indeed, because each Voronoi domain is restricted to within the open hemisphere centered at the generating point, the sets $\text{Vor}(x) \cap \text{Cap}_\eta(x)$ form a system in which every common intersection is either empty or contractible. The Nerve Theorem thus applies, proving that the subcomplex of the Delaunay mosaic has the same homotopy type as the union of caps of radius η . This property breaks down for the boundary complex of $\text{conv} X$. This can be seen by considering the four points on \mathbb{S}^2 shown in Figure 2: $A, B = (\pm\varepsilon, 0, \sqrt{1 - \varepsilon^2})$ and $C, D = (0, \pm 1/2, \sqrt{3}/2)$, in which ε is a sufficiently small positive real number. The great-circle arc shared by the Voronoi domains of C and D has length only slightly shorter than π and it intersects the union of four caps of geodesic radius η slightly larger than $\frac{\pi}{2}$ in two disconnected segments. The union of the four caps has the topology of a disk, while the nerve has the topology of a circle. Indeed, the latter consists of two triangles glued along a shared edge plus another edge connecting the two respective third vertices of the two triangles.

Poisson point process. We are interested in sets $X \subseteq \mathbb{S}^n$ that are randomly generated. In particular, we use a (stationary) *Poisson point process* with *density* $\rho > 0$, which is characterized by the following two properties:

1. the numbers of points in a finite collection of pairwise disjoint Borel sets on \mathbb{S}^n are independent random variables;
2. the expected number of points in a Borel set is ρ times the Lebesgue measure of the set.

See [11] for an introduction to Poisson point processes. The two conditions imply that the probability of having k points in a Borel set $B \subseteq \mathbb{S}^n$ with Lebesgue measure $\|B\|$ is $\mathbb{P}[|X \cap B| = k] = \rho^k \|B\|^k e^{-\rho \|B\|} / k!$. In particular, the probability of having no point in B is $\mathbb{P}[X \cap B = \emptyset] = e^{-\rho \|B\|}$. It is not difficult to prove that the realization X of a Poisson point process on \mathbb{S}^n is finite and in general position with probability 1, a property we will assume for the remainder of this paper. It follows that $\text{Del}X$ is an n -dimensional simplicial complex and, by Lemma 4, that $\mathcal{R}: \text{Del}X \rightarrow \mathbb{R}$ is a generalized discrete Morse function.

To familiarize ourselves with the definition of a Poisson point process, we prove that the difference between the boundary complex of $\text{conv } X$ and $\text{Del}X$ is small. More precisely, the number of faces of $\text{conv } X$ that are visible from 0 outside $\text{conv } X$ vanishes rapidly as the density increases. This is consistent with the rapid decrease of the probability that $0 \notin \text{conv } X$, as computed by Wendel [25] for the uniform distribution on \mathbb{S}^n .

► **Lemma 5 (Non-Delaunay Faces).** *Let X be a Poisson point process with density $\rho > 0$ on \mathbb{S}^n . For every $0 \leq k \leq n$, the expected number of k -faces of $\text{conv } X$ that do not belong to $\text{Del}X$ goes to 0 as ρ goes to ∞ .*

Proof. We may assume that $\text{conv } X$ is simplicial and that no $n+1$ points lie on a great-sphere of \mathbb{S}^n . Let $Q \subseteq X$ be a set of $n+1$ points and consider its small and big caps. The big cap has volume larger than $\sigma_{n+1}/2$, and Q is a facet of $\text{conv } X$ but not a simplex of $\text{Del}X$ iff this big cap is empty. The probability of this event is less than $e^{-\rho\sigma_{n+1}/2}$. The expected number of such facets of $\text{conv } X$ is therefore less than a constant times $\rho^{n+1}e^{-\rho\sigma_{n+1}/2}$, which goes to 0 as ρ goes to ∞ . Here we used that $\mathbb{E}[|X|^{n+1}]$ is at most a constant times ρ^{n+1} . For $k < n$, every k -face of $\text{conv } X$ that does not belong to $\text{Del}X$ is a face of a facet with this property. The expected number of such k -faces thus also goes to 0 as ρ goes to ∞ . ◀

4 Proof of Main Result

In this section, we prove the main result of this paper stated as Theorem 1 in the Introduction. It consists of an integral equation for the expected number of intervals as a function of the maximum geodesic radius, and an asymptotic version of the formula for $\rho \rightarrow \infty$.

4.1 The Integral Equation

We begin with the proof of the integral equation, (5). The main tools are the Slivnyak–Mecke formula, which we will discuss shortly, and the Blaschke–Petkantschin formula for the sphere, which was stated and proved in Section 2. In addition, we employ the combinatorial analysis of inscribed simplices in [6].

The Slivnyak–Mecke approach. In a nutshell, the *Slivnyak–Mecke formula* writes the expectation of a random variable of a Poisson point process as an integral over the space on which the process is defined; see [23, page 68]. To write this integral, we recall that $\mathbf{x} = (x_0, x_1, \dots, x_k)$ is a sequence of $k+1$ points or k -simplex on \mathbb{S}^n , that $\mathbb{P}_\emptyset: (\mathbb{S}^n)^{k+1} \rightarrow \mathbb{R}$ maps \mathbf{x} to the probability that its smallest circumscribed cap is empty, that $\mathbf{1}_{k-\ell}: (\mathbb{S}^n)^{k+1} \rightarrow \mathbb{R}$ indicates whether or not the number of facets visible from the Euclidean center of the smallest circumscribed cap is $k-\ell$, and that $\mathbf{1}_\eta: (\mathbb{S}^n)^{k+1} \rightarrow \mathbb{R}$ indicates whether or not $\mathcal{R}(\mathbf{x}) \leq \eta$. Choosing points from a Poisson point process with density $\rho > 0$ on \mathbb{S}^n , we use Slivnyak–Mecke to write the expected number of intervals of type (ℓ, k) and geodesic radius at most η_0 as

$$\mathbb{E}[c_{\ell,k}^n, \eta_0] = \frac{\rho^{k+1}}{(k+1)!} \int_{\mathbf{x} \in (\mathbb{S}^n)^{k+1}} \mathbb{P}_\emptyset(\mathbf{x}) \cdot \mathbf{1}_{k-\ell}(\mathbf{x}) \cdot \mathbf{1}_{\eta_0}(\mathbf{x}) \, d\mathbf{x}, \quad (34)$$

in which $0 \leq \ell \leq k \leq n$; compare with [6]. The probability that the smallest circumscribed cap of the k -simplex is empty is $\mathbb{P}_\emptyset(\mathbf{x}) = e^{-\rho \text{Area}(\eta)}$, with η the geodesic radius of the cap. To compute the integral in (34), we apply Equation (10) from Theorem 3 with $f(\mathbf{x}) = \mathbb{P}_\emptyset(\mathbf{x}) \mathbf{1}_{k-\ell}(\mathbf{x}) \mathbf{1}_{\eta_0}(\mathbf{x})$. The corresponding function from the statement of Theorem 3,

$f_r : (\mathbb{S}^{k-1})^{k+1} \subseteq (\mathbb{R}^{n+1})^{k+1} \rightarrow \mathbb{R}$, is defined by $f_r(\mathbf{u}) = \mathbb{P}_\emptyset(r) \mathbf{1}_{k-\ell}(\mathbf{u}) \mathbf{1}_{\eta_0}(r)$, where we write $\mathbb{P}_\emptyset(r) = \mathbb{P}_\emptyset(\mathbf{u})$ and $\mathbf{1}_{\eta_0}(r) = \mathbf{1}_{\eta_0}(\mathbf{u})$ to emphasize that these expressions depend only on the radius. Equation (10) then gives

$$\begin{aligned} \int_{\mathbf{x} \in (\mathbb{S}^n)^{k+1}} f(\mathbf{x}) \, d\mathbf{x} &= \frac{\sigma_{n+1}}{2} \|\mathcal{L}_k^n\| \int_{t=0}^1 t^{\frac{kn-2}{2}} (1-t)^{\frac{n-k-1}{2}} \mathbb{P}_\emptyset(\sqrt{t}) \mathbf{1}_{\eta_0}(\sqrt{t}) \\ &\quad \times \int_{\mathbf{u} \in (\mathbb{S}^{k-1})^{k+1}} \mathbf{1}_{k-\ell}(\mathbf{u}) [k! \text{Vol}(\mathbf{u})]^{n-k+1} \, d\mathbf{u} \, dt. \end{aligned} \quad (35)$$

Substitution and reformulation. To continue, we recall $E_{\ell,k}^n = \mathbb{E}[\text{Vol}(\mathbf{u})^{n-k+1} \mathbf{1}_{k-\ell}(\mathbf{u})]$ from (4), in which the expectation is for sampling $k+1$ points from the uniform distribution on \mathbb{S}^{k-1} . It follows that the second integral on the right-hand side of (35) is $k!^{n-k+1} \sigma_k^{k+1} E_{\ell,k}^n$. Rewriting (34) using (35), we therefore get

$$\mathbb{E}[c_{\ell,k}^n, \eta_0] = \frac{\rho^{k+1}}{(k+1)!} \frac{\sigma_{n+1}}{2} \|\mathcal{L}_k^n\| k!^{n-k+1} \sigma_k^{k+1} E_{\ell,k}^n \int_{t=0}^s t^{\frac{kn-2}{2}} (1-t)^{\frac{n-k-1}{2}} \mathbb{P}_\emptyset(\sqrt{t}) \, dt, \quad (36)$$

$$= \rho \sigma_{n+1} \cdot \frac{\sigma_n^k}{2\Gamma(k)n^{k-1}} \cdot C_{\ell,k}^n \int_{t=0}^s \rho^k t^{\frac{kn-2}{2}} (1-t)^{\frac{n-k-1}{2}} \mathbb{P}_\emptyset(\sqrt{t}) \, dt, \quad (37)$$

in which we absorb one indicator by limiting the range of integration to the square of the maximum Euclidean radius, $s = \sin^2 \eta_0$. To get (37) from (36), we cancel $k!$, move ρ^k inside the integral, and use (4) to substitute $[\sigma_n^k / (\Gamma(k)n^{k-1})] \cdot C_{\ell,k}^n$ for $[\|\mathcal{L}_k^n\| k!^{n-k} \sigma_k^{k+1} / (k+1)] \cdot E_{\ell,k}^n$. This proves the integral equation (5) in Theorem 1.

4.2 The Asymptotic Result

We continue with the proof of the asymptotic result (6). We proceed in two stages, first taking liberties and leaving gaps in the argument, and second filling all the gaps.

Argument with gaps. We are interested in the behavior of the integral in (37), when $\rho \rightarrow \infty$. We observe that the probability of a cap to be empty vanishes rapidly with increasing geodesic radius: $\mathbb{P}_\emptyset(r) = e^{-\rho \text{Area}(\eta)}$, in which $r = \sin \eta$ is the Euclidean radius. This implies that the integrand is concentrated in the vicinity of 0. To make sense of the radius in the limit, we re-scale by mapping η and ρ to the normalized radius, $\bar{\eta} = \eta \rho^{1/n}$. To proceed with the informal computations, we assume that η is close to 0 and prepare two approximations and one relation:

- A. the squared Euclidean radius is roughly the squared geodesic radius: $s = \sin^2 \eta \approx \eta^2$;
- B. the square of the height is $1 - s \approx 1$, which allows us to simplify the incomplete Beta function:

$$B_s\left(\frac{n}{2}, \frac{1}{2}\right) = \int_{t=0}^s t^{\frac{n}{2}-1} (1-t)^{-\frac{1}{2}} \, dt \approx \int_{t=0}^s t^{\frac{n}{2}-1} \, dt = \frac{2}{n} s^{n/2}; \quad (38)$$

- C. the relation $\frac{\sigma_{n+1}}{\sigma_n} = B\left(\frac{n}{2}, \frac{1}{2}\right)$ implies $\frac{\sigma_{n+1}}{n} / B\left(\frac{n}{2}, \frac{1}{2}\right) = \frac{\sigma_n}{n} = \nu_n$.

Returning to the integral in (5), but without the factor ρ^n , we get

$$\int_{t=0}^{\sin^2 \eta_0} t^{\frac{kn-2}{2}} (1-t)^{\frac{n-k-1}{2}} \mathbb{P}_\emptyset(\sqrt{t}) \, dt \approx \int_{t=0}^{\bar{\eta}_0^2 / \rho^{2/n}} t^{\frac{kn-2}{2}} e^{-\rho \nu_n t^{n/2}} \, dt, \quad (39)$$

in which we approximate the upper limit of the integration using A, and drop the middle factor because it is close to 1 according to B. The probability of having an empty cap is $\mathbb{P}_\emptyset(r) = e^{-\rho \text{Area}(\eta)}$, in which the area of the cap can be written in terms of Beta functions:

$$\text{Area}(\eta) = \frac{\sigma_{n+1} B_s(n/2, 1/2)}{2B(n/2, 1/2)} \approx \frac{\sigma_{n+1} (2/n) s^{n/2}}{2B(n/2, 1/2)} = \nu_n s^{n/2}, \quad (40)$$

using B for the approximation and C to get the final result, which we plug into the left-hand side of (39) to get the approximation on its right-hand side. The exponential term motivates us to change variables with $\tau = \rho \nu_n t^{n/2}$. Plugging $t = \tau^{2/n} / (\rho \nu_n)^{2/n}$ and $dt = [\frac{2}{n} \tau^{2/n-1} / (\rho \nu_n)^{2/n}] d\tau$ into the right-hand side of (39), we get

$$\int_{\tau=0}^v \tau^{k-1} (\rho \nu_n)^{-k} \left(\frac{2}{n}\right) e^{-\tau} d\tau = \frac{2n^{k-1}}{\rho^k \sigma_n^k} \cdot \gamma(k; v), \quad (41)$$

in which the upper bound of the integration range is $v = \rho \nu_n (\bar{\eta}_0^2 / \rho^{2/n})^{n/2} = \bar{\eta}_0^n \nu_n$, the power of τ is $\frac{2}{n} \frac{kn-2}{2} + \frac{2}{n} - 1 = k - 1$, and the power of $\rho \sigma_n$ is $-\frac{2}{n} \frac{kn-2}{2} - \frac{2}{n} = -k$. We get the right-hand side of (41) from the left-hand side using $\frac{\sigma_n}{n} = \nu_n$ and $\gamma(k; v) = \int_{\tau=0}^v \tau^{k-1} e^{-\tau} d\tau$. Finally plugging the right-hand side into (5), we get

$$\mathbb{E}[c_{\ell,k}^n, \eta_0] = \rho \sigma_{n+1} \cdot \frac{\sigma_n^k}{2\Gamma(k)n^{k-1}} \cdot C_{\ell,k}^n \int_{t=0}^{\sin^2 \eta_0} \rho^k t^{\frac{kn-2}{2}} (1-t)^{\frac{n-k-1}{2}} \mathbb{P}_\emptyset(\sqrt{t}) dt \quad (42)$$

$$= \rho \sigma_{n+1} \cdot \frac{\gamma(k; v)}{\Gamma(k)} \cdot C_{\ell,k}^n + o(\rho), \quad (43)$$

as claimed in Theorem 1. Making the unjustified substitution $v = \bar{\eta}_0^n \nu_n = \infty$, we get

$$\mathbb{E}[c_{\ell,k}^n] = \rho \sigma_{n+1} \cdot C_{\ell,k}^n + o(\rho), \quad (44)$$

as claimed in Remark (1C) after Theorem 1.

Formal justifications. We continue with the justification of the asymptotic equivalences claimed above. To recall, there is the approximation in (39) and the substitution $\bar{\eta}_0 = \infty$ after (43). Fixing a real number $0 \leq \delta \leq 1$, we introduce some notation to streamline the computations:

$$\alpha = \frac{kn-2}{2}, \quad \alpha' = \frac{n-k-1}{2}, \quad \beta = \frac{n}{2}, \quad \beta' = \frac{1}{2}, \quad c = \frac{\sigma_n}{2}, \quad (45)$$

$$g(s) = c \int_{t=0}^s t^{\beta-1} (1-t)^{\beta'-1} dt, \quad (46)$$

$$J_0 = \rho^k \int_{t=0}^1 t^\alpha (1-t)^{\alpha'} e^{-\rho g(t)} dt, \quad J_1(\delta) = \rho^k \int_{t=0}^\delta t^\alpha (1-t)^{\alpha'} e^{-\rho g(t)} dt, \quad (47)$$

$$J_2(\delta) = \rho^k \int_{t=0}^\delta t^\alpha e^{-\rho g(t)} dt, \quad J_3(\delta) = \rho^k \int_{t=0}^\delta t^\alpha e^{-\rho \frac{c}{\beta} t^\beta} dt. \quad (48)$$

We note that $\alpha, \alpha' \geq -\frac{1}{2}$, $\beta, \beta' \geq \frac{1}{2}$, and $g(s)$ is $c = \frac{\sigma_n}{2}$ times the incomplete Beta function. Recall that $\frac{\sigma_{n+1}}{\sigma_n} = B(\frac{n}{2}, \frac{1}{2})$, which implies that $g(s)$ is $\frac{\sigma_{n+1}}{2}$ times the ratio of incomplete over complete Beta functions. Hence $g(s) = \text{Area}(\eta)$, in which $s = \sin^2 \eta$; see (2). Note also that J_0 is the integral in (37) except that the integration range goes all the way to 1, which corresponds to computing the number of intervals without restricting the radius. For $\delta = 1$, we have $J_1 = J_0$, and for $\delta = \sin^2 \eta_0$, J_1 is ρ^k times the expression on the left-hand side of (39). Finally, for $\delta = \bar{\eta}_0^2 \rho^{-1/\beta}$, J_3 is the integral on the right-hand side of (39), which we computed in (41). Next, we list a sequence of observations:

I. The integral in (46) satisfies

$$\frac{c}{\beta} s^\beta \leq g(s) = c \int_{t=0}^s t^{(n-2)/2} (1-t)^{-1/2} dt \leq \frac{c}{\beta} s^\beta + \text{const} \cdot s^{\beta+1}, \quad (49)$$

for $0 \leq s \leq 1$ on the left, and for $0 \leq s \leq \frac{1}{2}$ on the right. Indeed, we have $1 \leq 1/\sqrt{1-t}$ for all $0 \leq t \leq 1$ and $1/\sqrt{1-t} \leq 1 + \text{const} \cdot t$ for all $0 \leq t \leq \frac{1}{2}$.

II. The absolute difference between J_0 and $J_1(\delta)$ satisfies

$$|J_0 - J_1(\delta)| = \rho^k \int_{t=\delta}^1 t^\alpha (1-t)^{\alpha'} e^{-\rho g(t)} dt \leq \rho^k e^{-\rho \frac{c}{\beta} \delta^\beta} B(\alpha+1, \alpha'+1), \quad (50)$$

because $g(t) \geq g(\delta)$ throughout the integration domain, and $g(\delta) \geq \frac{c}{\beta} \delta^\beta$ by I. The value of the Beta function is a constant independent of ρ .

III. For $\delta \leq \frac{1}{2}$, the absolute difference between J_1 and J_2 satisfies

$$|J_1(\delta) - J_2(\delta)| \leq \rho^k \int_{t=0}^\delta [t^\alpha (1-t)^{\alpha'} - t^\alpha] e^{-\rho g(t)} dt \leq \text{const} \cdot \delta J_2(\delta), \quad (51)$$

because $|1 - (1-t)^{\alpha'}| \leq \text{const} \cdot t$ for all $0 \leq t \leq \frac{1}{2}$ and $\alpha' \geq -\frac{1}{2}$.

IV. For $\delta \leq \frac{1}{2}$, the absolute difference between J_2 and J_3 satisfies

$$|J_2(\delta) - J_3(\delta)| = \rho^k \int_{t=0}^\delta t^\alpha [e^{-\rho \frac{c}{\beta} t^\beta} - e^{-\rho g(t)}] dt \quad (52)$$

$$\leq \rho^k \int_{t=0}^\delta t^\alpha e^{-\rho \frac{c}{\beta} t^\beta} [1 - e^{-\text{const} \cdot \rho t^{\beta+1}}] dt \quad (53)$$

$$\leq J_3(\delta) [1 - e^{-\text{const} \cdot \rho \delta^{\beta+1}}], \quad (54)$$

in which we use the left inequality in I to get the right order of the exponential terms in (52), and the right inequality in I to get (53).

V. For $\eta \leq 1/\sqrt{2}$, the absolute difference between J_1 at the values $\sin^2 \eta$ and η^2 satisfies

$$|J_1(\sin^2 \eta) - J_1(\eta^2)| = \rho^k \int_{t=\sin^2 \eta}^{\eta^2} t^\alpha (1-t)^{\alpha'} e^{-\rho g(t)} dt \leq 2\rho^k \int_{t=\sin^2 \eta}^{\eta^2} t^\alpha dt \quad (55)$$

$$\leq \frac{2\rho^k}{\alpha+1} [\eta^{2\alpha+2} - (\eta - \eta^2)^{2\alpha+2}] \leq 4\rho^k \eta^{2\alpha+3}, \quad (56)$$

in which we use $(1-t)^{\alpha'} \leq 2$ for $t \leq \frac{1}{2}$ to get the right-hand side of (55). We use $\sin \eta > \eta - \eta^2$, which we glean from the Taylor series $\sin \eta = \eta - \frac{1}{6}\eta^3 + \dots$, and the binomial expansion of $(\eta - \eta^2)^{2\alpha+2}$ to get (56).

As mentioned earlier, $J_1(\sin^2 \eta_0)$ is ρ^k times the left-hand side of (39), and $J_3(\eta_0^2)$ is ρ^k times the right-hand side of (39). According to (41), ρ^k times this right-hand side is $(2n^{k-1}/\sigma_n^k) \cdot \gamma(k; v)$, with $v = \bar{\eta}^n \nu_n$, which is a positive constant; see Remark (1B) where we first mentioned that this integral is bounded from 0 as well as from ∞ . Having established that there is a positive constant $C = J_3(\eta_0^2)$, IV implies that $J_2(\eta_0^2) \leq C + (1 - e^{-\rho \frac{c}{\beta} \eta_0^{2(\beta+1)}})C$ is also bounded by a constant. Using III, IV, V, we get

$$|J_1(\sin^2 \eta_0) - J_3(\eta_0^2)| \leq |J_1(\sin^2 \eta_0) - J_1(\eta_0^2)| + |J_1(\eta_0^2) - J_2(\eta_0^2)| + |J_2(\eta_0^2) - J_3(\eta_0^2)| \quad (57)$$

$$\leq 4\rho^k \eta_0^{2\alpha+3} + \text{const} \cdot \eta_0^2 J_2(\eta_0^2) + (1 - e^{-\text{const} \cdot \rho \eta_0^{2(\beta+1)}})C. \quad (58)$$

Letting ρ to to infinity, we observe

$$\rho^k \bar{\eta}_0^{2\alpha+3} = \rho^k \left(\bar{\eta}_0 \rho^{-\frac{1}{n}} \right)^{kn+1} \rightarrow 0, \quad (59)$$

$$\rho \bar{\eta}_0^{2(\beta+1)} = \rho \left(\bar{\eta}_0 \rho^{-\frac{1}{n}} \right)^{n+2} \rightarrow 0, \quad (60)$$

implying the three terms in (58) go to 0. This finally justifies the approximation (39) and the argument proving Theorem 1.

Justification of Remark (1C). We finally prove that we can compute J_0 by setting $\bar{\eta}_0$ to infinity in (43) or, more formally, by replacing the incomplete gamma function in the expression by the complete gamma function. Such a justification is needed because so far we have treated the geodesic radius as a constant in our computations. We now couple the bound of the integration domain with the density by setting $\delta_0 = \rho^{-1/(\beta+1/2)}$. We reuse Equations (39) and (43) to compute $J_3(\delta_0) = (2n^{k-1}/\sigma_n^k) \cdot \gamma(k; v)$, with $v = \rho \nu_n \delta_0^{n/2} = \nu_n \rho^{1/(n+1)}$. The upper bound for the incomplete Gamma function thus goes to infinity and approaches the complete Gamma function. We still have $J_3(\delta_0)$ bounded by a constant, so the rest of the argument above goes through. We finally use II, which shows $|J_0 - J_1(\delta_0)| \rightarrow 0$. This justifies (44) and Remark (1C) in the Introduction.

5 Discussion

The main result of this paper is a radius-dependent integral equation for the expected number of intervals of the radius function of a Poisson point process on \mathbb{S}^n . To first order, the expected numbers are the same as in \mathbb{R}^n ; compare with [6]. The Delaunay mosaics on \mathbb{S}^n relate to inscribed convex polytopes in \mathbb{R}^{n+1} and to the Delaunay mosaics in the standard n -simplex equipped with the Fisher information metric. These diagrams have therefore very similar stochastic properties as the Delaunay mosaics in \mathbb{R}^n . We formulate a few questions that are motivated by the findings reported in this article.

- As mentioned earlier, the first-order terms of the expected number of intervals of the radius function do not distinguish \mathbb{S}^n from \mathbb{R}^n . There are no further terms in the Euclidean case, but what are they for \mathbb{S}^n ?
- Projecting the convex hull of a finite $X \subseteq \mathbb{S}^n$ orthogonally onto a $(k+1)$ -plane corresponds to slicing the Voronoi tessellation of X with a k -dimensional great-sphere of \mathbb{S}^n . Similarly, we can define a k -dimensional weighted Delaunay mosaic by slicing a Voronoi tessellation in \mathbb{R}^n with a k -plane. What are the stochastic properties of these slices and projections?
- The square of the Fisher information metric agrees infinitesimally with the Kullback–Leibler divergence [12]. The more general class of Bregman divergences has recently come into focus [7]. What are the stochastic properties of the Bregman divergences and their corresponding metrics? Is the similarity to the Euclidean metric specific to the Fisher information metric or is it a more general phenomenon?

Acknowledgements

The authors thank Matthias Reitzner for sharing a draft on Poisson–Delaunay mosaics on the sphere, Žiga Virk and Hubert Wagner for their help in connecting this work with Fisher information space, and Nicholas Barton for pointing out that the connection has been discovered earlier by Antonelli.

References

- 1 E. AKIN. *The Geometry of Population Genetics*. Springer, Berlin, 1979.
- 2 S. AMARI AND H. NAGAOKA. *Methods of Information Geometry*. Amer. Math. Soc., Providence, Rhode Island, 2000.
- 3 P.L. ANTONELLI ET AL. The geometry of random drift I-VI. *Adv. Appl. Prob.* **9-12** (1977-80).
- 4 I. BÁRÁNY, F. FODOR AND V. VÍGH. Intrinsic volumes of inscribed random polytopes in smooth convex bodies. *Adv. Appl. Prob. (SGSA)* **42** (2010), 605–619.
- 5 U. BAUER AND H. EDELSBRUNNER. The Morse theory of Čech and Delaunay complexes. *Trans. Amer. Math. Soc.*, to appear.
- 6 H. EDELSBRUNNER, A. NIKITENKO AND M. REITZNER. Expected sizes of Poisson–Delaunay mosaics and their discrete Morse functions. Manuscript, IST Austria, Klosterneuburg, Austria, 2016.
- 7 H. EDELSBRUNNER AND H. WAGNER. Topological data analysis with Bregman divergences. In “Proc. 33rd Ann. Symp. Comput. Geom., 2017”, to appear.
- 8 R. FORMAN. Morse theory for cell complexes. *Adv. Math.* **134** (1998), 90–145.
- 9 E. HEWITT AND K. STROMBERG. *Real and Abstract Analysis*. Springer, Berlin, Germany, 1965.
- 10 D. HUG. Random polytopes. In: *Stochastic Geometry, Spatial Statistics and Random Fields*, ed.: E. Spodarev, Lecture Notes in Mathematics **2068**, Springer, Heidelberg, 2013, 205–238.
- 11 J.F.C. KINGMAN. *Poisson Processes*. Oxford Univ. Press, Oxford, England, 1993.
- 12 S. KULLBACK AND R.A. LEIBLER. On information and sufficiency. *Amer. Math. Stat.* **22** (1951), 79–86.
- 13 J. LERAY. Sur la forme des espaces topologiques et sur les points fixes des représentations. *J. Math. Pures Appl.* **24** (1945), 95–167.
- 14 S. LI. Concise formulas for the area and volume of a hyperspherical cap. *Asian J. Math. Stat.* **4** (2011), 66–70.
- 15 R.E. MILES. Poisson flats in Euclidean spaces. Part I: a finite number of random uniform flats. *Adv. Appl. Prob.* **1** (1969), 211–237.
- 16 R.E. MILES. On the homogeneous planar Poisson point process. *Math. Biosci.* **6** (1970), 85–127.
- 17 R.E. MILES. Isotropic random simplices. *Adv. Appl. Prob.* **3** (1971), 353–382.
- 18 J. MØLLER. Random tessellations in \mathbb{R}^d . *Adv. Appl. Prob.* **21** (1989), 37–73.
- 19 M. REITZNER. Random polytopes. In: *New Perspectives in Stochastic Geometry*, eds.: W.S. Kendall and I. Molchanov, Oxford Univ. Press, 2010, 45–76.
- 20 M. REITZNER AND J. STEMESEDER. Expected number of faces of random polytopes with vertices on the boundary of a smooth convex body. Manuscript, Math. Dept., Univ. Osnabrück, Germany, 2016.
- 21 R.J. RENKA. Algorithm 772: STRIPACK: Delaunay triangulation and Voronoi diagram on the surface of a sphere. *ACM Trans. Math. Software* **23** (1997), 416–434.
- 22 R. SCHNEIDER. Recent results on random polytopes. *Boll. Unione Mat. Ital.* **1** (2008), 17–39.
- 23 R. SCHNEIDER AND W. WEIL. *Stochastic and Integral Geometry*. Springer, Berlin, Germany, 2008.
- 24 J. STEMESEDER. Random polytopes with vertices on the sphere. Ph.D. Thesis, Math. Dept., Univ. Salzburg, Austria, 2014.
- 25 J.G. WENDEL. A problem in geometric probability. *Math. Scand.* **11** (1962), 109–111.
- 26 M. ZÄHLE. A kinematic formula and moment measures of random sets. *Mathematische Nachrichten* **149** (1990), 325–340.

A Uniform Distribution

In this appendix, we sketch the case of the uniform distribution on \mathbb{S}^n . The sole difference to the Poisson point process is that the number of points is prescribed rather than a random variable. Setting this number to $N = \rho\sigma_{n+1}$, it makes sense that in the limit, when N and ρ go to infinity, the expected numbers of intervals of the radius function are the same under both probabilistic models. This is indeed what we establish now more formally. By linearity of expectation, the number of intervals of type (ℓ, k) and geodesic radius at most η_0 is

$$\mathbb{E}[c_{\ell,k}^n, \eta_0] = \binom{N}{k+1} \mathbb{E}[\mathbb{P}_\emptyset(\mathbf{x}) \cdot \mathbf{1}_{k-\ell}(\mathbf{x}) \cdot \mathbf{1}_{\eta_0}(\mathbf{x})], \quad (61)$$

in which $\mathbf{x} = (x_0, x_1, \dots, x_k)$ is a sequence of $k+1$ points on \mathbb{S}^n , η is the geodesic radius of the smallest circumscribed cap of \mathbf{x} , and $\mathbb{P}_\emptyset(\mathbf{x}) = (1 - \text{Area}(\eta)/\sigma_{n+1})^{N-k+1}$ is the probability that this cap is empty. The analogue of (34) is therefore

$$\mathbb{E}[c_{\ell,k}^n, \eta_0] = \binom{N}{k+1} \frac{1}{\sigma_{n+1}^{k+1}} \int_{\mathbf{x} \in (\mathbb{S}^n)^{k+1}} \mathbb{P}_\emptyset(\mathbf{x}) \cdot \mathbf{1}_{k-\ell}(\mathbf{x}) \cdot \mathbf{1}_{\eta_0}(\mathbf{x}) \, d\mathbf{x}. \quad (62)$$

We apply the rotation-invariant Blaschke–Petkantschin formula (10), again with narrow bump functions as in (35). This gives

$$\mathbb{E}[c_{\ell,k}^n, \eta_0] = \frac{N!}{(N-k-1)! \sigma_{n+1}^k} \frac{\sigma_n^k}{2\Gamma(k)n^{k-1}} \cdot C_{\ell,k}^n \int_{t=0}^{\sin^2 \eta_0} t^{\frac{k-2}{2}} (1-t)^{\frac{n-k-1}{2}} \left(1 - \frac{\text{Area}(\eta)}{\sigma_{n+1}}\right)^{N-k+1} dt, \quad (63)$$

in which $\eta = \eta(t) = \arcsin \sqrt{t}$; compare with (37). To prepare the next step, we note that

$$\left(1 - \frac{\text{Area}(\eta(t))}{\sigma_{n+1}}\right)^{N-k+1} \approx e^{-\frac{N}{\sigma_{n+1}} \text{Area}(\eta(t))} \quad (64)$$

as $t \rightarrow 0$. From here on, we retrace the steps we took from (39) to (41). In particular, we change variables with $\tau = \frac{N}{\sigma_{n+1}} \nu_n t^{n/2}$, and we substitute $\bar{\eta}_0 \rho^{-1/n}$ for η_0 . Observing $\frac{N!}{(N-k-1)!} \approx N^{k+1}$, we simplify the expression and get

$$\mathbb{E}[c_{\ell,k}^n, \bar{\eta}_0] = N \cdot \frac{\gamma(k;v)}{\Gamma(k)} \cdot C_{\ell,k}^n + o(N) \quad (65)$$

for the expected number of intervals of the radius function of the Delaunay mosaic for N points chosen uniformly at random on \mathbb{S}^n , in which $v = \bar{\eta}_0^n \nu_n$. Comparing with the asymptotic result (6) in Theorem 1, we see the same constants as for the Poisson point process. However, the variance distinguishes the two cases, being smaller for the uniform distribution than for the Poisson point process; see [24].